Inorg. Chem. **2008**, *47*, 8859−8868

Inorganic Chemistry
Article

Magneto-Structure Relationship in Copper(II) and Nickel(II) Complexes Chelated with Stable *tert*-Butyl 5-Phenyl-2-pyridyl Nitroxide and Related Radicals

Atsushi Okazawa,[†,‡] Yasunori Nagaichi,[†] Takashi Nogami,[†] and Takayuki Ishida*[,†,‡]

Department of Applied Physics and Chemistry and Course of Coherent Optical Science, The University of Electro-Communications, Chofu, Tokyo 182-8585, Japan

Received May 23, 2008

We have isolated and characterized a new paramagnetic bidentate ligand, *tert*-butyl 5-phenyl-2-pyridyl nitroxide (phpyNO). The spin distribution onto the pyridine ring was clarified from the Electron Spin Resonance spectrum. Complexation of phpyNO with nickel(II) and copper(II) ions gave ML_2-type chelated compounds. The magnetic measurements of $[Ni(phpyNO)_2(H_2O)_2]\cdot(ClO_4)_2$ and $[Cu(phpyNO)_2(H_2O)]\cdot(ClO_4)_2\cdot C_6H_4Cl_2$ revealed that the metal-radical exchange couplings were ferromagnetic with $2J/k_B = +409(10)$ and $+434(12)$ K, respectively. The torsion angle (ϕ) around $M-O-N-C_{2py}$ can be regarded as a reliable indicator for the plane geometry of chelates; namely, highly planar chelates defined by small ϕ exhibit ferromagnetic coupling. An approximate linear relation was found in the J versus ϕ plot using the data of the present complexes and related known compounds. The critical angle of ϕ, at which the sign of the metal-radical exchange changes from positive to negative, was 12.6(9)°. This finding could be almost reproduced by density-functional theory calculation on a model copper(II)-nitroxide dyad. The exchange couplings in equatorially coordinated copper(II)- and nickel(II)-nitroxide complexes are very strongly ferromagnetic by nature.

Introduction

Metal-radical hybrid solids have been well investigated for molecule-based magnets, where a radical center is directly bonded to the metal ion, affording considerably large magnetic exchange coupling.[1] Various 2-pyridyl-substituted ligands containing a paramagnetic $S = 1/2$ center such as nitronyl nitroxide (NN) groups[2−4] have been known to form chelate rings (see Scheme 1 for their structural formulas). We have proposed *tert*-butyl 2-pyridyl nitroxide (2pyNO; NO stands for the *tert*-butyl nitroxide group)[5] as a promising candidate for such purpose. However, the simple pyridyl-NOs have been reported to be unisolable.[6]

Scheme 1. Structural Formulas

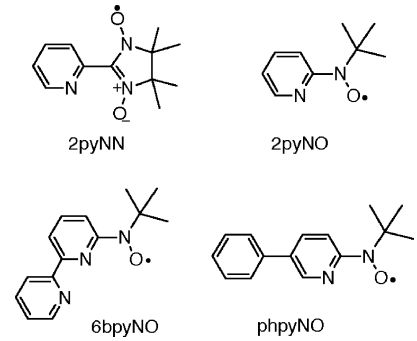

Thanks to the stabilization from an extended aromatic ring, 6bpyNO has been available for synthesis of $[Ni^{II}(6bpyNO)_2](PF_6)_2$ and $[Cu^{II}(6bpyNO)Cl_2]$,[7] both of which exhibited strong intramolecular ferromagnetic couplings with $2J/k_B =$

* To whom correspondence should be addressed. E-mail: ishi@pc.uec.ac.jp.
† Department of Applied Physics and Chemistry.
‡ Course of Coherent Optical Science.

(1) (a) Caneschi, A.; Gatteschi, D.; Sessoli, R.; Rey, P. *Acc. Chem. Res.* **1989**, *22*, 392. (b) Manriquez, J. M.; Yee, G. T.; McLean, R. S.; Epstein, A. J.; Miller, J. S. *Science* **1991**, *252*, 1415. (c) Inoue, K.; Hayamizu, T.; Iwamura, H.; Hashizume, D.; Ohashi, Y. *J. Am. Chem. Soc.* **1996**, *118*, 1803. (d) Lamaire, M. T. *Pure Appl. Chem.* **2004**, *76*, 277.
(2) Romero, F. M.; Luneau, D.; Ziessel, R. *Chem. Commun.* **1998**, 551.
(3) Aoki, C.; Ishida, T.; Nogami, T. *Inorg. Chem.* **2003**, *42*, 7616.
(4) (a) Luneau, D.; Rey, P.; Laugier, J.; Fries, P.; Caneschi, A.; Gatteschi, D.; Sessoli, R. *J. Am. Chem. Soc.* **1991**, *113*, 1245. (b) Luneau, D.; Rey, P.; Laugier, J.; Belorizky, E.; Conge, A. *Inorg. Chem.* **1992**, *31*, 3578.
(5) Okazawa, A.; Nogami, T.; Ishida, T. *Chem. Mater.* **2007**, *19*, 2733.
(6) Keana, J. F. W. *Chem. Rev.* **1978**, *78*, 37.

10.1021/ic800937n CCC: $40.75
Published on Web 08/27/2008

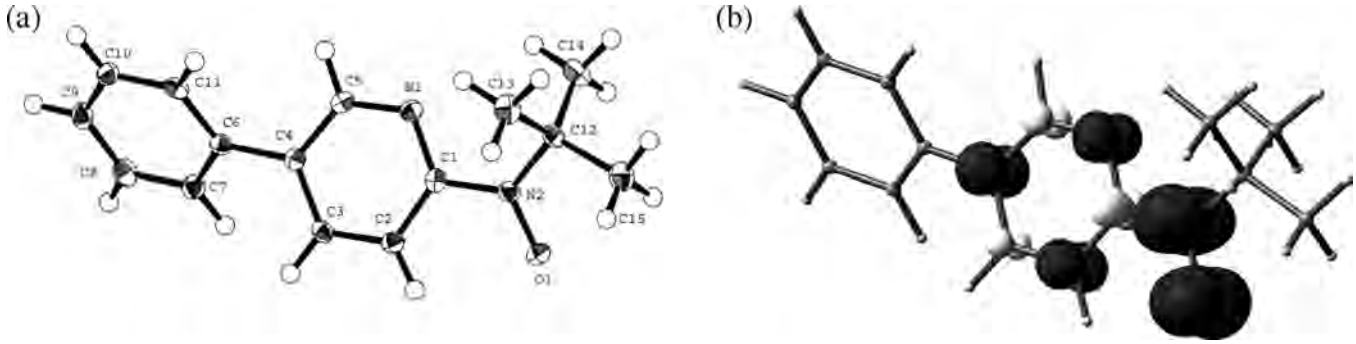

Figure 1. (a) Molecular structure of phpyNO with thermal ellipsoids at the 50% probability level for non-hydrogen atoms. (b) Spin density surface of phpyNO calculated at the DFT UB3LYP/6−311G(d,p)//UB3LYP/6−31G(d,p) level. Dark gray, positive spin; light gray, negative spin. The isocontour value is set to 0.004.

~400 K, where the exchange parameter is defined to be $-2J$. The ferromagnetic couplings are explained in terms of the orthogonality between the π^*-type singly occupied molecular orbital (SOMO) of the radical and the dσ-type SOMO(s) of nickel(II) ($3d^8$; $S_{Ni} = 1$) and copper(II) ions ($3d^9$; $S_{Cu} = 1/2$).[2−5,7,8] The mother skeleton 2pyNO should be handled much more delicately than 6bpyNO. The 2pyNO-chelated compounds were successfully synthesized by a trapping method with suitable transition metal ions, without isolation of 2pyNO.[5]

We propose here a new candidate, *tert*-butyl 5-phenyl-2-pyridyl nitroxide (abbreviated as phpyNO), as a paramagnetic ligand. An additional phenyl group at the pyridine 5-position will facilitate isolation because substitution at the para position with respect to the nitroxide radical group is quite effective for stabilization.[6,9] Actually, this modification enabled us to utilize phpyNO as an isolable synthetic intermediate. After a chelation reaction of phpyNO with copper(II) or nickel(II) ions, we determined the molecular structures by means of X-ray crystallographic analysis and evaluated magnetic couplings between nitroxide radical spins and copper(II) or nickel(II) spins. The relationship between the geometry and intramolecular metal-radical magnetic coupling will be discussed. There are many geometrical freedoms of the atoms involved in the chelate structure, and one may wonder what would be a good parameter for describing the orthogonal geometry. No simple magneto-structure relationship has been reported to date, including the works on nitronyl nitroxide ligands as well as nitroxide ones, before our work.[5,7] We will show a satisfactory relation by choosing a single geometrical parameter.

Results

Characterization of phpyNO. We synthesized and isolated a paramagnetic ligand, phpyNO. The precursory hydroxylamine phpyNOH was prepared according to the conventional method,[5,7,9] and the oxidation with Ag_2O gave phpyNO, which could be purified by passing through silica-gel column chromatography. The spectroscopic measurements of phpyNO satisfied the molecular formula. This compound crystallizes at room temperature under air, and the crystal structure was determined by means of X-ray diffraction study (Figure 1a). The nitroxide nitrogen atom is highly planar, whereas the hydroxylamine nitrogen atom pyramidalized. The N−O bond distance in phpyNO is 1.2900(15) Å, which is in a typical range for aromatic *tert*-butyl nitroxide,[10] and much shorter than the corresponding bond length in phpyNOH (1.4550(12) Å). Such a change of the N−O distance is important when we determine the nominal charge of the N−O group in the complexes of phpyNO and related compounds. The nitroxide oxygen atom is located at the transoid position with respect to the pyridine nitrogen atom, but the C1−N2 bond freely rotates during the complexation reaction.

The solution Electron Spin Resonance (ESR) spectra of phpyNO and 2pyNO[5] are shown in Figure 2. The phenyl group in phpyNO masks one of the proton splittings, but the ESR spectrum of phpyNO was not simplified, because additional hyperfine splittings took place from the phenyl protons. We analyzed the hyperfine splitting constants of phpyNO as well as those of 2pyNO (Figure 2b).

We estimated the spin distribution on the pyridine ring from the McConnell relation, $a_H = Q_C\rho_C$,[11] where ρ_C stands for spin density at the aromatic carbon atom connected with the proton (Table 1). We applied $Q_C = -2.45$ mT proposed for azaaromatic rings.[12] As for the pyridine nitrogen, a similar equation, $a_N = Q_N\rho_N$ with $Q_N = +2.5$ mT,[13] is available to estimate directly the spin density at the nitrogen atom (ρ_N). The sign could not be determined solely from the ESR data, but there have been many examples describing the spin-polarization[14] leading to alternating spin density on the

(7) Osanai, K.; Okazawa, A.; Nogami, T.; Ishida, T. *J. Am. Chem. Soc.* **2006**, *128*, 14008.
(8) Kahn, O.; Prins, R.; Reedijk, J.; Thompson, J. S. *Inorg. Chem.* **1987**, *26*, 3557.
(9) (a) Calder, A.; Forrester, A. R. *J. Chem. Soc. C* **1969**, 1459. (b) Forrester, A. R.; Hepburn, S. P. *J. Chem. Soc., Perkin I* **1974**, 2208.
(10) (a) Nishimaki, H.; Mashiyama, S.; Yasui, M.; Nogami, T.; Ishida, T. *Chem. Mater.* **2006**, *18*, 3602. (b) Inoue, K.; Iwamura, H. *Adv. Mater.* **1992**, *4*, 801. (c) Fujita, J.; Tanaka, M.; Suemune, H.; Koga, N.; Matsuda, K.; Iwamura, H. *J. Am. Chem. Soc.* **1996**, *118*, 9347.
(11) (a) McConnell, H. M.; Strathdee, J. *Mol. Phys.* **1959**, *2*, 129. (b) McConnell, H. M. *J. Chem. Phys.* **1958**, *28*, 1188.
(12) Talcott, C. L.; Myers, R. J. *Mol. Phys.* **1967**, *12*, 549.
(13) Carrington, A.; dos Santos-Veiga, J. *Mol. Phys.* **1962**, *5*, 21.
(14) (a) Iwamura, H. *Adv. Phys. Org. Chem.* **1990**, *26*, 179. (b) Rajca, A. *Chem. Rev.* **1994**, *94*, 871. (c) Ishida, T.; Iwamura, H. *J. Am. Chem. Soc.* **1991**, *113*, 4238. (d) Mataga, N. *Theor. Chim. Acta* **1967**, *10*, 372. (e) Longuet-Higgins, J. C. *J. Chem. Phys.* **1950**, *18*, 265.

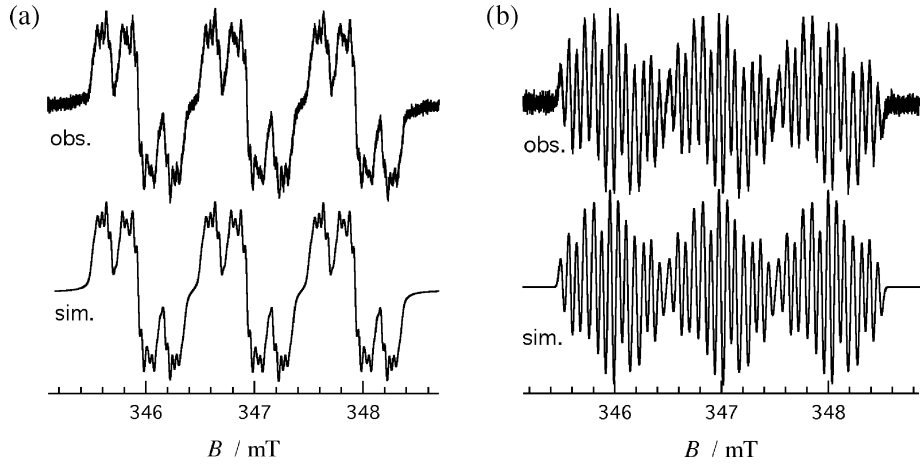

Figure 2. X-band ESR spectra of (a) phpyNO and (b) 2pyNO in toluene at room temperature. Simulated spectra are also drawn.

Table 1. Observed Hyperfine Splitting Constants, Spin Densities, and Calculated Spin Densities for phpyNO and 2pyNO

compounds		a_X /mT[a]		ρ_C, ρ_N (experiments)[b]	ρ_C, ρ_N (calculation)[c]
phpyNO	$a_{N(NO)}$	1.000			0.340
	$a_{N(py)}$	0.143	$\rho_{N(py)}$	0.057	0.113
	$a_{H3(py)}$	0.240	$\rho_{C3(py)}$	0.099	0.125
	$a_{H4(py)}$	0.080	$\rho_{C4(py)}$	(−)0.033	−0.056
	$a_{H6(py)}$	0.080	$\rho_{C6(py)}$	(−)0.033	−0.059
	$a_{H(o,p\text{-ph})}$	0.037	$\rho_{C(o,p\text{-ph})}$	0.015	0.020[d]
2pyNO	$a_{N(NO)}$	1.023			0.345
	$a_{N(py)}$	0.143	$\rho_{N(py)}$	0.057	0.090
	$a_{H3(py)}$	0.243	$\rho_{C3(py)}$	0.099	0.114
	$a_{H4(py)}$	0.070	$\rho_{C4(py)}$	(−)0.031	−0.054
	$a_{H5(py)}$	0.243	$\rho_{C5(py)}$	0.099	0.119
	$a_{H6(py)}$	0.070	$\rho_{C6(py)}$	(−)0.031	−0.057

[a] Measured in toluene at room temperature. The g values were 2.0060 and 2.0061 for phpyNO and 2pyNO, respectively. [b] Estimated from the McConnell relations, $a_N = Q_N\rho_N$ with $Q_N = +2.5$ mT for pyridine nitrogen atoms and $a_H = Q_C\rho_C$ with $Q_C = -2.45$ mT for pyridine carbon atoms. Negative signs are assumed from the spin-polarization scheme. [c] DFT calculation at the UB3LYP/6−311G(d,p) level after geometries were optimized at the UB3LYP/6−31G(d,p) level. [d] Averaged on those of two ortho and one para positions.

aromatic groups including pyridines.[15] DFT (density-functional theory) calculations supported the determination of the sign (Figure 1b for phpyNO), in which the geometry was optimized because the experimental data were obtained in a solution, and the magnitudes are also consistent with the experiments (Table 1). The polarized spin density calculated by DFT was slightly overestimated compared with those of the ESR results.

Crystal Structure Analysis of the Copper(II) and Nickel(II) Complexes. Because phpyNO has a π^*-type SOMO as illustrated in Figure 1b, we focused our attention on transition metal ions having dσ-type magnetic orbitals, such as nickel(II) and copper(II) ions, to bestow the orthogonal arrangement between them at the direct nitroxide-metal bond. Actually, we prepared several chelated compounds with phpyNO according to a method similar to those of the 2pyNO[5] and 6bpyNO complexes.[7] Simply mixing of phpyNO with divalent metal salts in appropriate organic solvents gave polycrystals of ML_2-type compounds: $[Ni(phpyNO)_2(H_2O)_2]\cdot(ClO_4)_2$ (**1**), $[Cu(phpyNO)_2(ClO_4)_2]\cdot 2CH_2Cl_2$ (**2**), $[Cu(phpyNO)_2(H_2O)]\cdot(ClO_4)_2\cdot C_6H_4Cl_2$ (**3**), and $[Cu(phpyNO)_2(CF_3SO_3)_2]\cdot 0.35H_2O$ (**4**). They were characterized by means of elemental analysis and IR spectroscopy, and finally their molecular structures were successfully determined by means of X-ray crystallographic analysis (Figure 3 and Tables 2 and 3).

We can find five-membered chelate rings involving a nitroxide group in every compound. In the molecule of **1** (Figure 3a), two water molecules occupy the axial position with respect to the chelate plane, and the counteranion ClO_4^- is located at the clearance in the crystal. A 2_1 screw axis runs through O2−Ni1−O3. The N1−O1 bond length is 1.306(3) Å, supporting that the phpyNO ligand is paramagnetic. The Ni−O and −N distances of 1.981(2)−2.078(3) Å imply an octahedral structure with $S_{Ni} = 1$. The planar chelate ring guarantees the orthogonal arrangement between nickel dσ orbitals (i.e., $3d_{x^2-y^2}$ and $3d_{z^2}$) and nitroxide π^* orbital. We have proposed that the torsion angle along $M-O-N-C_{2py}$ is convenient as an indicator of the planar character.[3] The Ni1−O1−N2−C1 torsion angle in **1** is very small (1.5(3)°).

The molecule of **2** has an inversion center at the metal ion in the space group $P\bar{1}$ (Figure 3b). The crystal solvent molecules (dichloromethane) were incorporated in the clearance. Two perchlorate ions are coordinated at the axial positions, like $[Cu(2pyNO)_2(ClO_4)_2]$.[5] The Jahn−Teller distortion is found as usual; the copper(II) ion forms an elongated octahedron with the somewhat long axial Cu1−O2 distance (2.492(6) Å), compared with the equatorial Cu1−O1 and Cu1−N1 bonds. The Cu1−O1−N2−C1 torsion angle remains relatively small (−4.2(8)°), in comparison with that of $[Cu(2pyNO)_2(ClO_4)_2]$ (25.9(5)°).[5] This geometry indicates the approximate orthogonal arrangement between copper dσ orbital ($3d_{x^2-y^2}$) and nitroxide π^* orbital in **2**.

In the preparation of **2**, a minor impurity was found from one batch, and accordingly pure **2** could be manually picked up under a microscope and subjected to crystallographic analysis. From the elemental analysis on a bulk specimen, the ML_2-composition was unequivocally confirmed, but the

(15) (a) Kumada, H.; Sakane, A.; Koga, N.; Iwamura, H. *J. Chem. Soc., Dalton Trans.* **2000**, 911. (b) Shimada, T.; Ishida, T.; Nogami, T. *Polyhedron* **2005**, *24*, 2593. (c) Kitano, M.; Ishimaru, Y.; Inoue, K.; Koga, N.; Iwamura, H. *Inorg. Chem.* **1994**, *33*, 6012. (d) Ishimaru, Y.; Kitano, M.; Kumada, H.; Koga, N.; Iwamura, H. *Inorg. Chem.* **1998**, *37*, 2273.

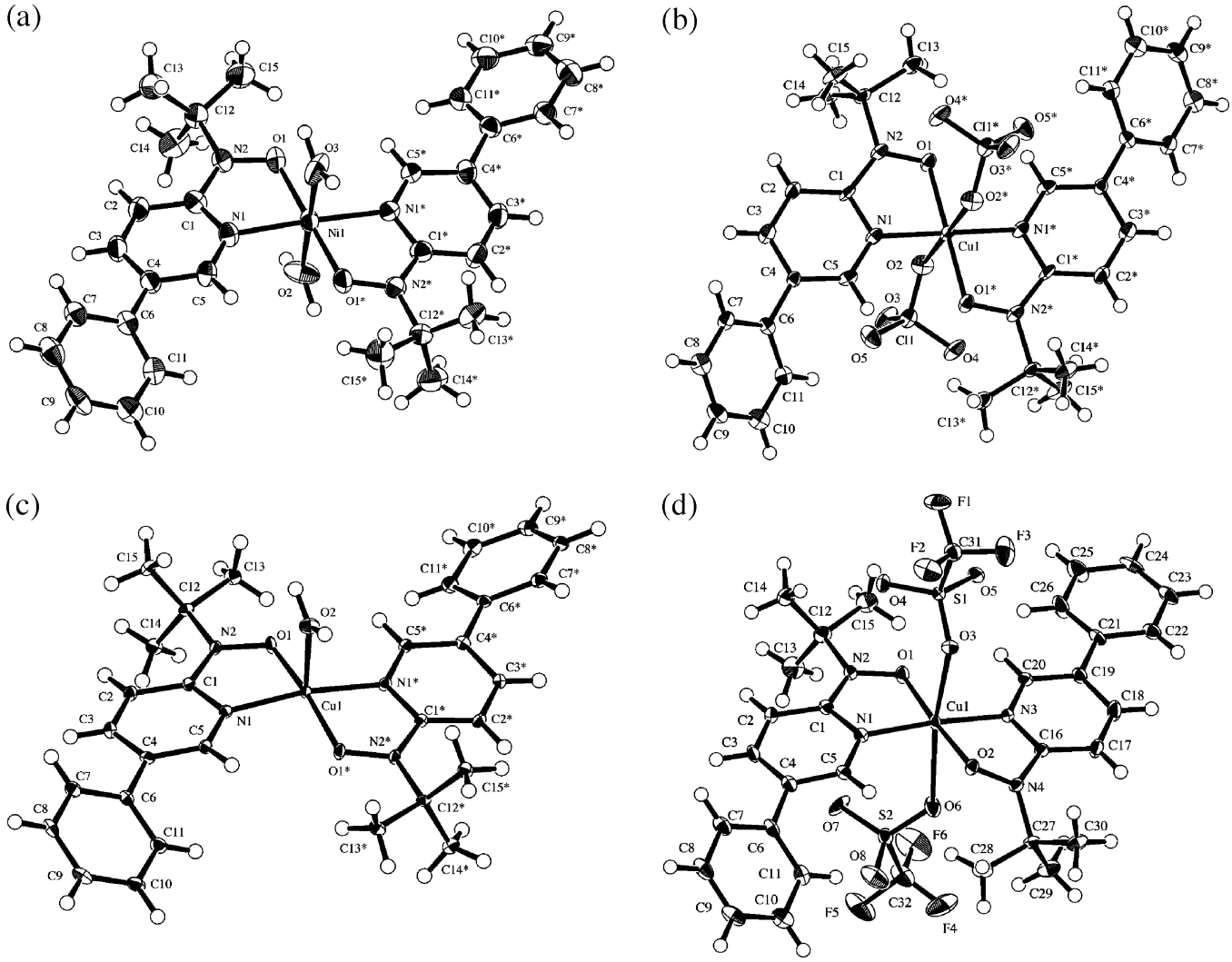

Figure 3. Molecular structures of (a) $[Ni(phpyNO)_2(H_2O)_2]^{2+}$ in **1**, (b) $[Cu(phpyNO)_2(ClO_4)_2]$ in **2**, (c) $[Cu(phpyNO)_2(H_2O)]^{2+}$ in **3**, and (d) $[Cu(phpyNO)_2(CF_3SO_3)_2]$ in **4** with thermal ellipsoids at the 50% probability level for non-hydrogen atoms. Atom numbering schemes are also shown. Only a major conformer is shown in (d).

Table 2. Selected Bond Lengths (Å) and Angles for **1**−**3**

compounds	**1**	**2**	**3**
M1−O1	1.981(2)	1.934(3)	1.9481(13)
M1−N1	2.035(2)	1.939(4)	1.961(2)
M1−O2	2.078(3)	2.492(6)	2.146(2)
M1−O3	2.071(3)		
O1−N2	1.306(3)	1.301(6)	1.309(3)
N2−C1	1.403(4)	1.404(5)	1.399(3)
O1−M1−N1	79.64(10)	81.69(16)	80.81(7)
M1−O1−N2	114.56(18)	113.2(2)	114.66(11)
O1−N2−C1	118.0(2)	117.7(4)	128.918(3)
O1−M1−O2	90.35(8)	92.24(18)	96.62(5)
N1−M1−O2	87.69(8)	87.7(2)	96.15(5)
O1−M1−O3	89.65(8)		
N1−M1−O3	92.31(8)		
M1−O1−N2−C1	1.5(3)	−4.2(8)	−1.6(2)
N1−M1−O1−N2	−4.7(2)	0.4(4)	1.65(14)
O2−M1−O1−N2	82.9(2)	87.7(4)	−93.54(13)
O3−M1−O1−N2	−97.1(2)		

Table 3. Selected Bond Lengths (Å) and Angles for **4**

Cu1−O1	1.9316(19)	Cu1−O2	1.9491(18)
Cu1−N1	1.9281(19)	Cu1−N3	1.9459(19)
Cu1−O3	2.4314(16)	Cu1−O6	2.5922(18)
N2−O1	1.304(2)	N4−O2	1.303(2)
N2−C1	1.391(3)	N4−C16	1.400(3)
N1−Cu1−O1	81.83(8)	N3−Cu1−O2	80.69(7)
Cu1−O1−N2	113.96(15)	Cu1−O2−N4	110.32(14)
O1−N2−C1	116.6(2)	O2−N4−C16	114.54(19)
O1−Cu1−O3	89.92(6)	O2−Cu1−O3	88.04(6)
O1−Cu1−O6	96.54(6)	O2−Cu1−O6	85.23(6)
Cu1−O1−N2−C1	−4.9(2)	Cu1−O2−N4−C16	33.4(2)
N1−Cu1−O1−N2	2.42(14)	N3−Cu1−O2−N4	−23.78(13)
O3−Cu1−O1−N2	−95.32(14)	O3−Cu1−O2−N4	−114.55(13)
O6−Cu1−O1−N2	89.96(14)	O6−Cu1−O2−N4	60.54(13)

ratio of the solvated molecules depended on the preparation batches. A preliminary crystal structure analysis of the impurity portion indicated the formula of $[Cu(phpyNO)_2(ClO_4)_2]\cdot 0.24CH_2Cl_2$ (**2′**) crystallized in a monoclinic *C*2/*c* space group as a pseudopolymorph. A somewhat distorted chelate ring was found as $\phi = 12.9(7)°$ after the refinement down to $R(F)$ ($I > 2\sigma(I)$) of 0.158.

To avoid the polymorph problem of **2** and **2′**, we tried to prepare and purify specimens from other solvents and finally found a good crystalline product (**3**) from 1,2-dichlorobenzene (Figure 3c). The copper ion in **3** has a square pyramid structure with a water molecule at an axial position. The Cu1−O2 distance (2.146(2) Å) is longer than those of

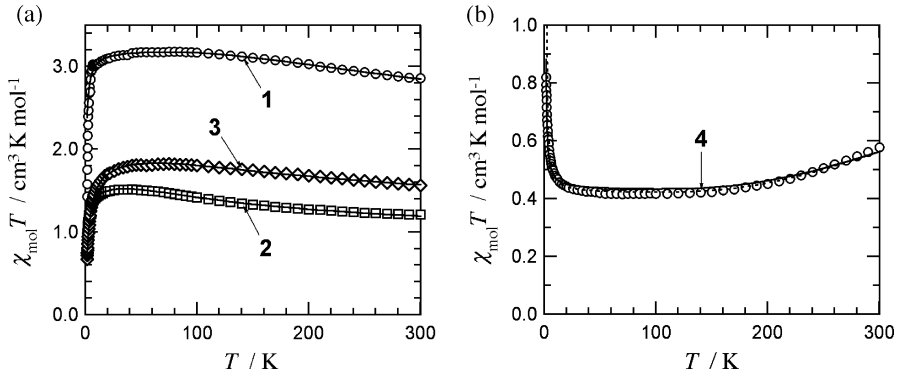

Figure 4. (a) Temperature dependence of $\chi_{mol}T$ for **1**−**3**. (b) Temperature dependence of $\chi_{mol}T$ for **4**. The applied magnetic fields were 500 Oe. The solid and dotted lines represent calculated curves. See the text for the equations and optimized parameters.

Table 4. Optimized Parameters, g_{avg}, J, and θ, Together with the Torsion Angle $|\phi|$ for **1**−**4** and Related Compounds

compounds[a]	g_{avg}	$2J\ k_B^{-1}$/K	θ /K	$\|\phi\|$ /deg	reference[b]
$[Ni(phpyNO)_2(H_2O)_2]\cdot(ClO_4)_2$ (**1**)	2.067(2)	+409(10)	−0.61(3)	1.5(3)	this work
$[Cu(phpyNO)_2(ClO_4)_2]\cdot 2CH_2Cl_2$ (**2**)	2.[c]	+276(4)	−1.18(1)	4.2(8)	this work
$[Cu(phpyNO)_2(H_2O)]\cdot(ClO_4)_2\cdot C_6H_4Cl_2$ (**3**)	2.035(4)	+434(12)	−2.92(4)	1.6(2)	this work
$[Cu(phpyNO)_2(CF_3SO_3)_2]\cdot 0.35H_2O$ (**4**)	2.139(8)	−940(30)[d]	+0.909(1)	33.4(2), 4.9(2)	this work
$[Ni(2pyNO)_2(H_2O)_2]\cdot(ClO_4)_2$	2.112(4)	+252(6)	−3.45(5)	3.9(3)	ref 5
$[Cu(2pyNO)_2(ClO_4)_2]$	2.064(2)	−548(4)[e]	+1.88(2)	25.9(5)	ref 5
$[Ni(6bpyNO)_2]\cdot(PF_6)_2$	2.082(1)	+384(4)	−0.67(1)	5.0(5)[f]	ref 7
$[Cu(6bpyNO)Cl_2]$	2.062(4)	+400(20)	−3.52(6)	10.7(2)	ref 7
$[Ni(4ImNNH)(NO_3)_2]$	2.06(1)	+85(3)	+1.04(3)	6.3(4)	ref 3
$[Cu(4ImNNH)(NO_3)_2]$	2.08(1)	−58(4)	0	15.6(4)	ref 3
$[Cu(4ImNNH)Br_2]$	2.05(1)	−372(5)	+1.69(7)	34.4(6)	ref 3
$[Ni(bpyNN_2)(H_2O)_2]\cdot(ClO_4)_2$	2.12	−140	−0.4	16.8	ref 27
$[Ni(bpyNN_2)(H_2O)(ClO_4)]\cdot(ClO_4)$	2.15	+80.0, +19.8	+1.0	8.1, 14.0	ref 27

[a] 4ImNNH and $bpyNN_2$ stand for 4-imidazolyl nitronyl nitroxide and 2,2′-bipyridine-6,6′-diyl bis(nitronyl nitroxide), respectively. [b] See Reference in the main text. [c] A purity factor was optimized to be 0.844(2) with the g_{avg} value fixed. [d] Another parameter was estimated as $2J/k_B = \sim+270$ K from the J vs $|\phi|$ relations with $\phi = 4.9(2)°$. [e] The J value in ref 5 should be corrected. [f] An averaged value on the geometries of four crystallographically independent units.

Cu1−O1 and Cu1−N1, and a 2-fold axis is located on the Cu1−O2 bond. The copper ion is slightly deviated from the basal plane as indicated with the O1−Cu1−O1* and N1−Cu1−N1* angles of 166.76(7) and 167.70(8)°, respectively. The chelate ring is highly planar with $\phi = 1.6(2)°$.

The molecular structure of **4** is unsymmetrical, and accordingly two nitoxide groups are crystallographically independent (Figure 3d). The space group is $P\bar{1}$, but the inversion center resides at the middle of two neighboring molecules. We found a disorder in the trifluoromethanesulfonate group involving S2 and C32. Their positions are related by a rotation around the Cu1−O6 with the optimized occupancy factors of 0.526(3)/0.474(3). Figure 3d shows a major conformation. The geometry of the chelate core does not show any disorder. The bond lengths around the copper ion (1.9281(19)−1.9491(18) Å) are close to those for **2** and **3**. Two torsion angles are −4.9(2) and 33.4(2)° for Cu1−O1−N2−C1 and Cu1−O2−N4-C16, respectively. The sterically bulky axial groups seem responsible for the deformation of the latter chelate ring, giving the severe torsion, while the former chelate ring remains highly planar. There is a solvated water molecule in a clearance with the optimized occupancy of 0.354(8).

Intramolecular Magnetic Coupling in 1−4. Magnetic susceptibilities of polycrystalline **1**−**4** were measured on a SQUID magnetometer. Upon cooling from 300 to 2 K, the $\chi_{mol}T$ values of **1**−**3** increased once, indicating the presence of intramolecular ferromagnetic interactions (Figure 4a). The spin-only values are 3.0 and 1.875 cm^3 K mol^{-1} for **1** ($S_{total} = 2$) and for **2** and **3** ($S_{total} = 3/2$), respectively. The $\chi_{mol}T$ values at their maximum clearly indicate that they have high-spin ground states. The final drops of the $\chi_{mol}T$ values are assigned to intermolecular antiferromagnetic couplings.

For **1**−**3**, the metal-radical interaction is unique owing to the 2-fold or inversion symmetry, and accordingly the Heisenberg spin-Hamiltonian was defined as $H = -2J(S_1\cdot S_2 + S_2\cdot S_3)$ for a three-centered system, in which coupling between the terminal ions was disregarded.[16,17] Thus, we applied the van Vleck equation to our systems, giving the following expressions, eqs 1 and 2 for the nickel(II) and copper(II) complexes, respectively.[18]

$$\chi_{mol} = \frac{2Ng_{avg}^2\mu_B^2}{k_B(T-\theta)} \times \frac{\exp(-2J/k_BT) + 1 + 5\exp(2J/k_BT)}{\exp(-4J/k_BT) + 3\exp(-2J/k_BT) + 3 + 5\exp(2J/k_BT)} \quad (1)$$

(16) (a) Bu, X.-H.; Tong, M.-L.; Xie, Y.-B.; Li, J.-R.; Chang, H.-C.; Kitagawa, S.; Ribas, J. *Inorg. Chem.* **2005**, *44*, 9837. (b) Lescouezec, R.; Lloret, F.; Julve, M.; Vaissermann, J.; Verdaguer, M. *Inorg. Chem.* **2002**, *41*, 818.
(17) (a) Bencini, A.; Benelli, C.; Dei, A.; Gatteschi, D. *Inorg. Chem.* **1985**, *24*, 695. (b) Tanaka, M.; Matsuda, K.; Iwamura, H. *J. Am. Chem. Soc.* **1998**, *120*, 7168.
(18) Gruber, S. J.; Harris, C. M.; Sinn, E. *J. Chem. Phys.* **1968**, *49*, 2183.

$$\chi_{mol} = \frac{N{g_{avg}}^2{\mu_B}^2}{4k_B(T-\theta)} \frac{\exp(-2J/k_BT) + 1 + 10\exp(J/k_BT)}{\exp(-2J/k_BT) + 1 + 2\exp(J/k_BT)} \quad (2)$$

The experimental data were fitted to these equations, and the parameters were optimized as summarized in Table 4. A Weiss mean field parameter θ was introduced for intermolecular antiferromagnetic couplings and also for the zero-field splitting of the nickel(II) ion in **1**. Because **2** (space group $P\bar{1}$) was contaminated with **2′** ($C2/c$), the purity factor p was defined and used for the molar fraction of **2**, on the assumption of the presence of a ground doublet species from **2′** as an $S = 1/2$ paramagnetic impurity.[19] The parameter p was optimized to be 0.844(2) with the g_{avg} value fixed to 2. The impurity contribution was relatively small in this measurement. The calculation fit was satisfactory (Figure 4a). The J value hardly depended on the variation of p, implying that obtained J value of **2** is reliable. There is no impurity problem in **3**, and we simply applied eq 2, giving the largest class of the J value ($2J/k_B = +434(12)$ K).

On the other hand, we characterized a ground low-spin state for **4** (Figure 4b). The experimental $\chi_{mol}T$ value of **4** decreased on cooling and reached to a plateau at $\chi_{mol}T = \sim 0.4$ cm^3 K mol^{-1} around 100 K, which is close to the spin-only $S_{total} = 1/2$ value. A final $\chi_{mol}T$ upsurge is assigned to intermolecular ferromagnetic coupling. We have to adopt an unsymmetrical model, $H = -2J_{12}S_1 \cdot S_2 - 2J_{23}S_2 \cdot S_3$, because the two terminal ions are crystallographically independent. We at first used eq 3 for the analysis of the magnetic data.[17]

$$\chi_{mol} = \frac{N{g_{avg}}^2{\mu_B}^2}{4k_B(T-\theta)} \times \frac{\exp(-2(J_{12}^2 + J_{23}^2 - J_{12}J_{23})^{1/2}/k_BT)) + 1 + 10\exp((J_{12} + J_{23} - (J_{12}^2 + J_{23}^2 - J_{12}J_{23})^{1/2})/k_BT)/\exp(-2(J_{12}^2 + J_{23}^2 - J_{12}J_{23})^{1/2}/k_BT) + 1 + 2\exp((J_{12} + J_{23} - (J_{12}^2 + J_{23}^2 - J_{12}J_{23})^{1/2})/k_BT)}{} \quad (3)$$

$$\chi_{mol} = \frac{N{g_{avg}}^2{\mu_B}^2}{k_B(T-\theta)}\left[\frac{1}{4} + \frac{2}{3 + \exp(-2J_{12}/k_BT)}\right] \quad (4)$$

We obtained negative J_{12} and positive J_{23} values for **4** from fitting with eq 3 and found the obtained J_{23} value accompanied by a large statistical error. The reason may reside in the strong S_1-S_2 pairing, leading to a trivial magnetic coupling between a doublet S_3 and a ground singlet S_1-S_2. In other words, J_{23} is insensitive to the $\chi_{mol}T$ versus T profile. Therefore, we utilized another equation consisting of a sum of a doublet term and a singlet−triplet equilibrium term[20] (eq 4), assuming the condition of $J_{23} \ll |J_{12}|$. The Weiss mean field parameter was introduced. The optimized $2J_{12}$ was −940(30) K with $\theta = +0.909(1)$ K (Table 4). The calculated

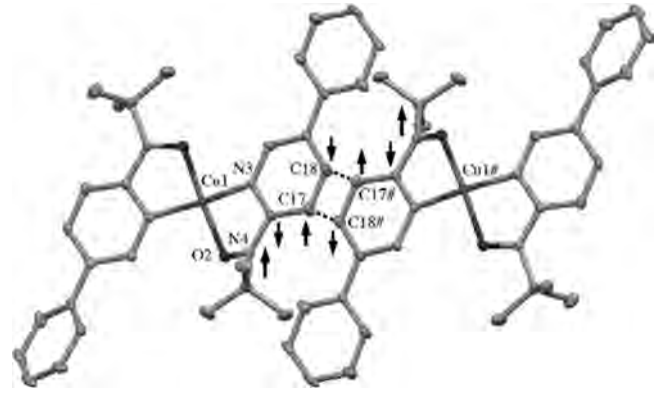

Figure 5. Molecular arrangement in the crystal of **4**. The axial ligands and hydrogen atoms are omitted for clarity. Dotted lines indicate the interatomic contacts of 3.594(3) Å between C17 and C18$^{\#}$, where the symmetry operation code of $^{\#}$ is $1-x, 1-y, z$. The possible spin polarization scheme is shown with arrows.

$\chi_{mol}T$ versus T curve reproduced well the experimental data as shown with the solid line in Figure 4b. Although we can not tell a priori which exchange interaction, J_{12} or J_{23}, of **4** would be assigned to each crystallographically independent copper-radical relation solely from the magnetic analysis, the negative one (J_{12}) is inferred to correspond to the largely twisted side (see below).

We have to mention briefly the intermolecular ferromagnetic coupling in the crystal of **4**. Figure 5 depicts a relatively short π-π type interaction between pyridine rings in neighboring molecules, which are related with centrosymmetry. The distance of C17 and C18$^{\#}$ (3.594(3) Å) is close to the sum of the van der Waals radii,[21] and the ferromagnetic coupling can be explained by the spin-polarization scheme[14,15,22,23] throughout the py—py contact (the arrows in Figure 5), since the pyridine ring in phyNO is appreciably spin-polarized, as evidenced by the ESR experiments. The weak intermolecular contact seems responsible for the small magnitude of the θ value.

Discussion

Magneto-Structure Relationship. We have found intramolecular metal-radical magnetic couplings varying in a considerably wide range from relatively small structural modifications. This family will lead to an insight into a detailed magneto-structure relationship. There are many parameters defining the mutual geometry around the radical N−O group and transition metal center. To simplify the discussion, we disregard several features commonly possessed by all of the compounds investigated here. The M−O distances range from 1.9316(19)−1.981(2) Å, and the M−O−N angles vary from 110.32(14)−114.66(11)°. The deviation of the axial ligand from the normal of the basal plane is indicated by the $O_{eq}-M-O_{ax}$ angles (85.23(6)−96.62(5)°). These parameters are basically important in the exchange coupling between the metal and nitroxide spins.

(19) The impurity **2′** might have a ground doublet state, because the torsion of **2′** was large (preliminarily 12.9(9)°). A negligibly interacting copper-radical relation seems possible as well. However, the ground quartet state of **2′** would give rise to an unrealistic g_{ave} value smaller than 2 as estimated from the somewhat small $\chi_{mol}T$ value.

(20) Bleaney, B.; Bowers, K. D. *Proc. R. Soc. London, Ser. A* **1952**, *214*, 451.

(21) Bondi, A. *J. Phys. Chem.* **1964**, *68*, 441.

(22) McConnell, H. M. *J. Chem. Phys.* **1963**, *39*, 1910.

(23) (a) Izuoka, A.; Murata, S.; Sugawara, T.; Iwamura, H. *J. Am. Chem. Soc.* **1985**, *107*, 1786. (b) Imachi, R.; Ishida, T.; Suzuki, M.; Yasui, M.; Iwasaki, F.; Nogami, T. *Chem. Lett.* **1997**, 743.

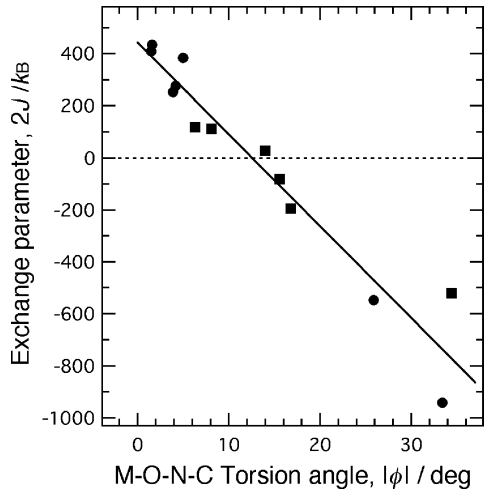

Figure 6. Plot of the observed exchange coupling parameter ($2J$) vs M−O−N−C_{2Ar} torsion angle ($|\phi|$) as a magneto-structure relationship in the nickel(II) or copper(II) complexes listed in Table 4. Circles and squares denote the data on the ArNO and ArNN complexes, respectively.

However, they made practically no difference in the magnetic coupling within a series of the present compounds. As we described above, the most important parameter is an indicator for the out-of-plane dislocation from the chelate ring with respect to the N−O−M moiety. We can regard the torsion around the M−O−N−C_{2py} skeleton as a representative of the geometry. The N_{py}−M−O−N torsion seems to be another candidate, but the former is more sensitive to the dislocation of the nitroxide O and N atoms from the chelate plane.

We can draw a plot of J versus $|\phi|$ for the copper(II) and nickel(II) complexes exhibiting equatorial chelation by nitroxide ligands (Figure 6). The copper(II) ion has a paramagnetic spin at $3d_{x^2-y^2}$, while the nickel(II) ion has two paramagnetic spins at $3d_{x^2-y^2}$ and $3d_{z^2}$. The $3d_{x^2-y^2}-\pi^*$ interaction dominantly contributes to the observed J, although $3d_{z^2}$ is orthogonal to π^* as well, viewing from the short distance and mutual lobe direction between interacting SOMOs. Therefore the interaction of $3d_{x^2-y^2}-\pi^*$ in the nickel(II) complexes is comparable to that of the copper(II) complexes, and their data are superposed in one plot. A significant pyramidalization around the copper(II) ion was observed in [Cu(6bpyNO)Cl_2], and its data point was omitted.

Furthermore, the present argument holds also for the chelates of nitronyl nitroxide radicals. The spin density on the oxygen atom of ArNO is assumed to be much larger than that of the ArNN, owing to an almost half size spin-delocalizable π-conjugation in the radical groups. More quantitative discussion needs the aid of the ESR study. The spin density at the ligating N−O oxygen atom is assumed to be approximately proportional to the a_N value of the nitroxide group. Typical a_N values of ArNO are 1.2 ± 0.2 mT,[24,25] while those of ArNN are 0.74 ± 0.03 mT[25a,26] (0.743 mT for phenyl NN in benzene[26] and 0.759 mT for 4-imidazolyl NN in toluene[3]). To superpose the data of the ArNN-based complexes in Figure 6, we multiplied the reported J values by a factor of 1.4 because the magnetic exchange coupling is proportional to the spin densities at the interacting atoms.[22] An advantage of the ArNO system over not only the ArNN system[27] but also the Ar-verdazyl[28] and Ar-dithiadiazolyl[29] ones (Scheme 2 for the molecular structures) can be pointed out. Their spins are delocalized mainly onto conjugated N_2O_2, N_4, and N_2S_2 systems, respectively, as clarified by the ESR hyperfine data (a_N etc.), while the spin in the NO group is highly localized in two atoms. Thus, strong exchange couplings were realized in the present ArNO system.

Scheme 2. Structural Formulas.

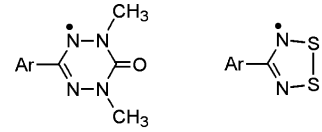

Ar-verydazyl Ar-dithiadiazolyl

Antiferromagnetic couplings were often observed in the copper(II) and nickel(II) coordination compounds chelated with 2-azaaromatic NN ligands.[3,27] The nickel(II) complex containing 2,2′-bipyridine-6,6′-diyl-bis(NN) (abbreviated as $bpyNN_2$ hereafter) exceptionally exhibited ferromagnetic coupling.[27] The tension operative in the fused 5- and 6-membered rings would regulate the M−O−N−C_{2Ar} structure to be more planar, like the case of the 6bpyNO complexes.[7] Luneau et al. discussed the coplanarity between the radical and metal equatorial planes but did not report the torsion angle (ϕ) around M−O−N−C_{2Ar}. We calculated these angles from their Supporting Information data; [Ni(bpyNN$_2$)(H$_2$O)$_2$](ClO$_4$)$_2$ showing $2J/k_B = -140$ and +114 K has M−O−N−C_{2Ar} torsion angles of 16.8 and 0.3° (the latter exhibited a severe structural disorder), and [Ni(bpyNN$_2$)(H$_2$O)(ClO$_4$)](ClO$_4$) showing $2J/k_B = +80.0$ and +19.8 K has M−O−N−C_{2Ar} torsion angles of 8.1 and 14.0° (Table 4). These data totally obeyed the relation presented here, as indicated with the superposition in Figure 6.

The magneto-structural relationship is simply formulated as $2J/k_B = a + b|\phi|$ with $a = 440(50)$ K and $b = -35(3)$ K deg^{-1} from Figure 6. The critical $|\phi|$, at which the sign of the metal-radical exchange coupling changes from positive to negative, is 12.6(9)°. Because an approximation (disregarding J_{23} in eq 4) was introduced in the analysis of the magnetic properties of **4** (see above), we reanalyze here the magnetic properties of **4** involving J_{23} in eq 3. The torsion

(24) (a) Calder, A.; Forrester, A. R.; Hepburn, S. P. *J. Chem. Soc., Perkin I* **1973**, 456. (b) Forrester, A. R.; Hepburn, S. P.; McConnachie, G. *J. Chem. Soc., Perkin I* **1974**, 2213.
(25) (a) Goldman, J.; Petersen, T. E.; Torssell, K.; Becher, J. *Tetrahedron* **1973**, *29*, 3833. (b) Lemaire, H.; Marechal, Y.; Ramasseul, R.; Rassat, A. *Bull. Soc. Chim. Fr.* **1965**, 372.
(26) Ullman, E. F.; Osiecki, J. H.; Boocock, G. B.; Darcy, R. *J. Am. Chem. Soc.* **1972**, *94*, 7049.
(27) Luneau, D.; Risoan, G.; Rey, P.; Grand, A.; Caneschi, A.; Gatteschi, D.; Laugier, J. *Inorg. Chem.* **1993**, *32*, 5616.
(28) (a) Hicks, R. G.; Lemaire, M. T.; Thompson, L. K.; Barclay, T. M. *J. Am. Chem. Soc.* **2000**, *122*, 8077. (b) Barclay, T. M.; Hicks, R. G.; Lemaire, M. T.; Thompson, L. K. *Chem. Commun.* **2000**, 2141. (c) Gilroy, J. B.; Koivisto, B. D.; McDonald, R.; Ferguson, M. J.; Hicks, R. G. *J. Mater. Chem.* **2006**, *16*, 2618.
(29) (a) Hearns, N. G. R.; Preuss, K. E.; Richardson, J. F.; Bin-Salamon, S. *J. Am. Chem. Soc.* **2004**, *126*, 9942. (b) Jennings, M.; Preuss, K. E.; Wu, J. *Chem. Commun.* **2006**, 341.

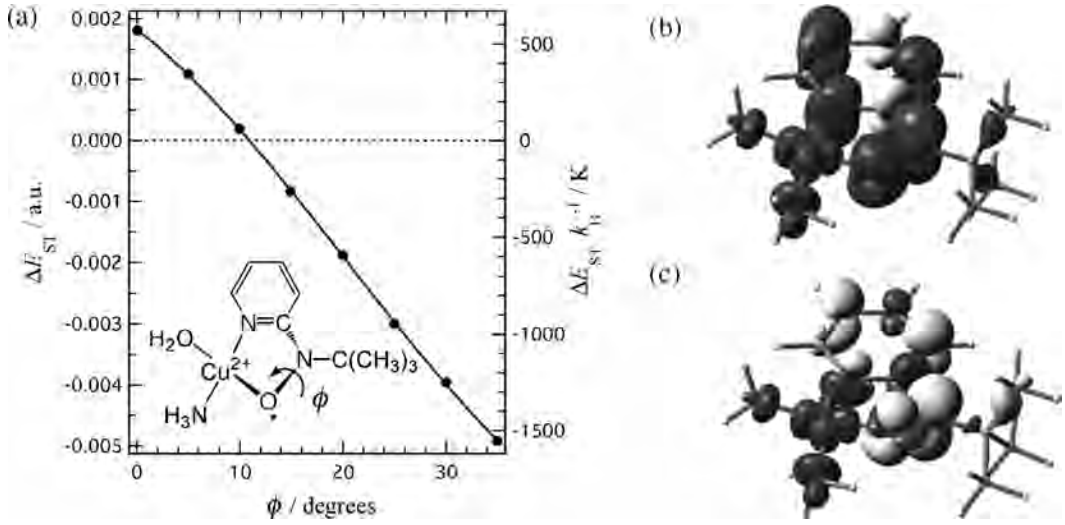

Figure 7. (a) DFT calculation result at the UB3LYP/6−311G(d,p)//HF/3−21G level of the singlet−triplet energy gap (ΔE_{ST}) as a function of the dihedral angle of Cu−O−N−C_{2py} (ϕ). A line is drawn as a guide to the eye. See the text for details. A model compound is also shown. (b) Spin density surfaces for the ground triplet state at $\phi = 0°$ and (c) for the ground singlet state at $\phi = 30°$. Dark gray, positive spin; light gray, negative spin.

of 4.9° leads to $2J_{23}/k_B = +270$ K from the relationship. The other parameters were optimized as $g_{avg} = 2.115(5)$, $2J_{12}/k_B = -964(14)$ K, and $\theta = +1.06(2)$ K, and the calculated $\chi_{mol}T$ versus T curve satisfactorily reproduced the experimental result (a dotted line in Figure 4b). The independently calculated values (−940(30) and −964(14) K) agree well with each other within a statistical error.

Finally, we confirmed this relation with a DFT MO calculation. A model molecule was proposed (Figure 7), in which peripheral substituents were simplified because of the reduction of the calculation cost, namely, a singlet−triplet equilibrium of $[Cu^{II}(2pyNO)(NH_3)(H_2O)]^{2+}$ was subjected to calculation. The molecular geometry was fully optimized, except for only one constraint (ϕ for the dihedral angle Cu−O−N−C_{2py}), at the HF/3−21G level. The energies of the singlet and triplet states were calculated at the UB3LYP/6−311G(d,p) level. The singlet−triplet energy gap ΔE_{ST} is plotted in Figure 7a, which corresponds to the experimental $2J$. We can find a monotonic decrease of ΔE_{ST} with an increase of ϕ. The critical angle of ϕ was calculated to be 10.9°.

Figures 7b and 7c display the spin density surfaces for the ground triplet model at $\phi = 0°$ and the ground singlet one at $\phi = 30°$, respectively. They qualitatively correspond to the SOMOs, and we confirm the σ- and π*-characters for the copper(II) and nitroxide SOMOs, respectively. The orthogonal arrangement of them is clearly demonstrated at $\phi = 0°$, while the violation of the orthogonality is pointed out at $\phi = 30°$. Moreover, we can imagine the strict orthogonal arrangement at $\phi = 180°$, as well as at $\phi = 0°$, by taking the symmetry of the oxygen $2p_z$ orbital into consideration. Therefore, the SOMO−SOMO overlap obeys cos 2ϕ (or $\cos^2 \phi$) dependence.[30] The curvature found in Figure 7a implies that an antiferromagnetic contribution (J_{AF}) in $J = J_F + J_{AF}$[31] mainly results from the SOMO−SOMO overlap.[32]

Note that the distances Cu−O, N−O and angles Cu−O−N, O−N−C_{2py} are entirely optimized under the condition of the single constraint of ϕ. Consequently this plot simply suggests that the dihedral angle is a good indicator for the magnetic coupling. The magnitude is a function of the interatomic Cu−O distances[33] which depend on bulkiness of the substituents. The DFT calculation tends to overestimate the exchange parameter;[34] in the present work, the calculation brought about J values larger than the experimental data by about 20% in the ferromagnetic region. The slope is not so reproducible with the experimental results. However, the critical angle between ferro- and antiferromagnetic couplings seems to be defined independent of the magnitude of J. The calculated value of 10.9° is close to the experimental one (12.6(9)°).

Concluding Remarks

It is well-known that axially coordinated copper(II)-nitroxide complexes exhibit ferromagnetic coupling,[1a,35] whereas equatorially coordinated copper(II)-niroxide complexes are often claimed to show antiferromagnetic coupling.[27,28] However, the present work informs us that the latter situation is potentially ferromagnetic as well; on the contrary, it is much more strongly ferromagnetic. A simple

(30) Venkataraman, L.; Klare, J. E.; Nuckolls, C.; Hyberstsen, M. S.; Steigerwald, M. L. *Nature* **2006**, *442*, 904.

(31) Kahn, O. *Molecular Magnetism*; VCH: New York, 1993; Chapter 9, p 145.

(32) The calculation curve does not exactly obey the cos 2ϕ law. The DFT optimized geometry of $[Cu^{II}(2pyNO)(NH_3)(H_2O)]^{2+}$ at $\phi = 0°$ was not planar at the copper center, as indicated with the N(py)−Cu−N(ammonia) and O(nitroxide)−Cu−O(water) angles of 167.8 and 168.3°, respectively. The J vs ϕ plot is not symmetrical with respect to $\phi = 0°$. The auxiliary coupling contribution due to the M−N(py) interaction to the total J is also responsible for the deviation from the pure cos 2ϕ dependence.

(33) Cervera, B.; Ruiz, R.; Lloret, F.; Julve, M.; Cano, J.; Faus, J.; Bois, C.; Mrozinski, J. *J. Chem. Soc., Dalton Trans.* **1997**, 395.

(34) (a) Dai, D.; Whangbo, M.-H.; Koo, H.-J.; Rocquefelte, X.; Jobic, S.; Villesuzanne, A. *Inorg. Chem.* **2005**, *44*, 2407. (b) Grau-Crespo, R.; de Leeuw, N. H.; Catlow, C. R. *J. Mater. Chem.* **2003**, *13*, 2848.

(35) (a) Benelli, C.; Gatteschi, D.; Carnegie, D. W., Jr.; Carlin, R. L. *J. Am. Chem. Soc.* **1985**, *107*, 2560. (b) Caneschi, A.; Gatteschi, D.; Laugier, J.; Rey, P. *J. Am. Chem. Soc.* **1987**, *109*, 2191.

Table 5. Selected Crystallographic Data for phpyNO and Complexes **1**−**4**

compounds	phpyNOH	phpyNO	**1**	**2**	**3**	**4**
formula	$C_{15}H_{18}N_2O$	$C_{15}H_{17}N_2O$	$C_{30}H_{38}Cl_2N_4NiO_{12}$	$C_{32}H_{38}Cl_6CuN_4O_{10}$	$C_{36}H_{40}Cl_4CuN_4O_{11}$	$C_{32}H_{34.7}CuF_6N_4O_{8.35}S_2$
crystal system	triclinic	monoclinic	orthorhombic	triclinic	monoclinic	triclinic
space group	$P\bar{1}$	$P2_1/c$	$C222_1$	$P\bar{1}$	$C2$	$P\bar{1}$
a/Å	6.435(4)	10.8007(3)	11.5278(7)	9.1578(2)	20.637(17)	10.762(6)
b/Å	9.750(6)	11.3559(3)	15.7492(10)	11.1366(15)	7.641(3)	11.551(5)
c/Å	11.898(8)	11.2283(3)	18.7820(14)	11.2967(13)	15.541(8)	14.984(13)
α/deg	66.99(5)	90	90	65.765(5)	90	87.84(4)
β/deg	87.11(5)	110.6004(13)	90	87.145(7)	128.918(3)	83.95(4)
γ/deg	77.42(5)	90	90	68.691(5)	90	82.14(4)
V/Å^3	670.2(7)	1289.11(6)	3409.9(4)	972.03(17)	1906.8(19)	1834.4(20)
Z	2	4	4	1	2	2
d_{cal}/g cm^{-3}	1.201	1.243	1.512	1.563	1.585	1.540
μ(Mo Kα)/mm^{-1}	0.076	0.079	0.793	1.033	0.919	0.797
R_{int}	0.082	0.076	0.097	0.100	0.040	0.048
R $(F)^a$ $(I > 2\sigma(I))$	0.0483	0.0383	0.0483	0.0727	0.0280	0.0438
$R_w(F^2)^b$ (all data)	0.0622	0.0351	0.0480	0.1043	0.0431	0.0667
GOF	1.072	0.970	1.035	1.193	1.010	1.134
unique reflections	3038	2941	3923	4199	4132	8335
T/K	110	100	104	110	90	90

^{a} $R = \sum||F_o| - |F_c||/\sum|F_o|$. ^{b} $R_w = [\sum w(F_o^2 - F_c^2)^2/\sum w(F_o^2)^2]^{1/2}$.

magneto-structure relationship has been proposed plausibly indicating that the critical ϕ value is 12.6(9)°. We can point out an advantage of the 5-membered chelation structure. Ferromagnetic coupling can often be obtained in the copper(II) and nickel(II) complexes involving 2pyNO-type radicals because of the highly planar 5-membered rings, in comparison with 6-membered rings. Intramolecular ferromagnetic couplings are thus designed on the basis of the SOMO−SOMO orthogonality.

The spin is appreciably polarized onto the pyridine ring, in contrast to the case of nitronyl nitroxide and other radicals.[36] The N_{py}−M coordination may play an auxiliary role in ferromagnetic interaction because the pyridine nitrogen atom is spin-polarized and the $2p_z$(N) orbital is orthogonal to $3d\sigma$(M). A few compounds are known to exhibit intermolecular ferromagnetic coupling[3,5] like **4**. We can expect intramolecular, as well as intermolecular, magnetic couplings through the pyridine rings being regarded as an advantage of the ArNO system over the NN system. Introduction of π-conjugated radicals seems promising, and the replacement of the bulky *tert*-butyl group with aromatic groups[37] is now underway.

Experimental Section

Materials. *N-tert*-Butyl N-(5-phenyl-2-pyridyl) hydroxylamine (phpyNOH). The precursor 2-bromo-5-phenylpyridine[38] was prepared from 2-bromo-5-pyridylboronic acid and iodobenzene by the Suzuki coupling reaction. To the toluene solution (150 mL) containing 2-bromo-5-phenylpyridine (2.67 g; 11.4 mmol) was added a hexane solution (1.61 mol/L) of butyl lithium (7.8 mL; 13 mmol) at −78 °C under nitrogen atmosphere. After the mixture was stirred at −78 °C for 0.5 h, a toluene solution (20 mL) containing 2-methyl-2-nitrosopropane (1.19 g; 13.7 mmol) was added to the above mixture at −78 °C. The mixture was stirred, being allowed to warm gradually up to room temperature. The reaction mixture was quenched by aqueous NH_4Cl and neutralized with aqueous $NaHCO_3$ at room temperature. The organic layer was separated, dried over anhydrous $MgSO_4$, filtered, and concentrated under reduced pressure. A main product was purified by passing through a short column (silica gel) with 1/1 dichloromethane-ether as an eluent. Recrystallization from dichloromethane/hexane gave 1.42 g of a colorless solid of phpyNOH (5.87 mmol; 52%). Mp. 99−101 °C. ^{1}H NMR (270 MHz, $CDCl_3$) δ 1.30 (s, 9H), 7.19 (dd, 1H, J = 9, 1 Hz), 7.38−7.58(m, 6H), 7.81 (dd, 1H, J = 9, 3 Hz), 8.57 (dd, 1H, J = 3, 1 Hz). ^{13}C NMR (68 MHz, $CDCl_3$) δ 26.5, 61.8, 117.0, 126.6, 127.5, 128.9, 132.0, 135.1, 137.3, 144.4, 160.9. These NMR data were recorded in the presence of a trace amount of phenylhydrazine.[39] MS (EI, 70 eV) m/z 241.9 (MH^+), 225.9, 210.9, 185.9, 169.9, 154.9. IR (KBr disk) 696, 758, 860, 1200, 1265, 1469, 1593, 2993, 3205 cm^{-1}.

***tert*-Butyl (5-phenyl-2-pyridyl) nitroxide (phpyNO).** Freshly prepared Ag_2O (579 mg) was added to a dichloromethane solution (20 mL) containing 121 mg (0.50 mmol) of phpyNOH, and the mixture was stirred at room temperature for 1 h. The supernatant immediately turned red. The solution phase was filtered and concentrated under reduced pressure. A main product was purified by passing a short column (silica gel; dichloromethane as an eluent). Red platelet crystals of phpyNO were obtained after the removal of the solvent. The yield was 88 mg (0.37 mmol; 73%). Mp. 87.5−88.5 °C. ESR (X-band, toluene, room temperature) g = 2.0060, see Table 1 for the hyperfine splitting constants. MS (ESI+) m/z 264.1 $(M + Na)^+$, 208.1 $(M - t\text{-Bu} + Na)^+$. IR (KBr disk) 698, 768, 849, 1190, 1265, 1377, 1462, 2989 cm^{-1}.

Coordination Compounds. A dichloromethane solution (1 mL) containing 48 mg (0.20 mmol) of phpyNO was combined with an ethanol solution (1 mL) containing 36 mg (0.10 mmol) of $Ni(ClO_4)_2 \cdot 6H_2O$, and the resultant solution was stirred for 1 min. A slow diffusion with ether gave dark purple crystals of **1**. After being kept in a refrigerator for 2 days, the crystals were separated on a filter and washed with ether. The yield was 62 mg (0.080 mmol; 80%). Single crystals suitable for the X-ray diffraction study were obtained by slow diffusion of ether into an acetone solution of **1**. Mp. 149−152 °C (decomp.). Anal. Calcd for

(36) (a) Zheludev, A.; Barone, V.; Bonnet, M.; Delley, B.; Grand, A.; Ressouche, E.; Rey, P.; Subra, R.; Schweizer, J. *J. Am. Chem. Soc.* **1994**, *116*, 2019. (b) Awaga, K.; Inabe, T.; Maruyama, Y. *Chem. Phys. Lett.* **1992**, *190*, 349.
(37) Okazawa, A.; Nogami, T.; Ishida, T. *Polyhedron* **2007**, *26*, 1965.
(38) Parry, P. R.; Wang, C.; Batsanov, A. S.; Bryce, M. R.; Tarbit, B. *J. Org. Chem.* **2002**, *67*, 7541.
(39) Lee, T. D.; Keana, J. F. W. *J. Org. Chem.* **1975**, *40*, 3145.

$C_{30}H_{38}Cl_2N_4NiO_{12}$ (i.e., $[Ni(phpyNO)_2(H_2O)_2]\cdot(ClO_4)_2$): C, 46.42; H, 4.93; N, 7.22%. Found: C, 46.36; H, 4.82; N, 7.21%. IR (KBr disk) 627, 696, 766, 1090, 1117, 1144, 1456, 2993, 3392 cm^{-1}.

Similarly, **2**, was prepared from phpyNO and $Cu(ClO_4)_2\cdot 6(H_2O)$ in 2/1 dichloromethane-ethanol as black needles of **2** in 63% yield. Mp. 140−141 °C (decomp.). Anal. Calcd for $C_{30.9}H_{35.8}Cl_{3.8}CuN_4O_{10}$ (i.e., $[Cu(phpyNO)_2(ClO_4)_2]\cdot 0.9CH_2Cl_2$): C, 45.18; H, 4.39; N, 6.82%. Found: C, 45.02; H, 4.52; N, 7.11%. IR (KBr disk) 627, 698, 768, 1090, 1117, 1146, 1458, 2985 cm^{-1}. The ratio of the solvated molecules depended on batches, owing to the presence of **2′** ($[Cu(phpyNO)_2(ClO_4)_2]\cdot 0.24CH_2Cl_2$) as an impurity.

Compound **3** was prepared from phpyNO and $Cu(ClO_4)_2\cdot 6(H_2O)$ in 1/2 *o*-dichlorobenzene-acetonitrile as black plates of **3** in 57% yield. Mp. 158−160 °C (decomp.). Anal. Calcd for $C_{36}H_{40}Cl_4CuN_4O_{11}$ (i.e., $[Cu(phpyNO)_2(H_2O)]\cdot(ClO_4)_2\cdot C_6H_4Cl_2$): C, 47.51; H, 4.43; N, 6.16%. Found: C, 47.39; H, 4.43; N, 6.39%. IR (KBr disk) 627, 698, 768, 1090, 1115, 1146, 1458, 2987, 3437 cm^{-1}.

Compound **4** was prepared from phpyNO and $Cu(CF_3SO_3)_2$ in 1/1 chloroform-acetonitrile as black block crystals in 71% yield. Mp 148−149 °C (decomp.). Anal. Calcd for $C_{32}H_{34.7}CuF_6N_4O_{8.35}S_2$ (i.e., $[Cu(phpyNO)_2(CF_3SO_3)_2]\cdot 0.35H_2O$): C, 45.18; H, 4.11; N, 6.59; S, 7.54%. Found: C, 45.02; H, 4.02; N, 6.79; S, 7.56%. IR (KBr disk) 638, 766, 1032, 1165, 1263, 1279, 1456, 2991, 3523 cm^{-1}.

Instruments. ESR Spectroscopy. ESR spectra of phpyNO and 2pyNO were recorded on a Bruker ESP300E X-band (9.7 GHz) spectrometer. After the sample solution in toluene was thoroughly purged with nitrogen, the ESR spectra were recorded immediately at room temperature. Simulated spectra were calculated in the WinEPR Simfonia.[40]

X-ray Crystal Structure Analysis. X-ray diffraction data of single crystals the specimens were collected on Rigaku R-axis RAPID and Saturn70 CCD diffractometers with graphite monochromated Mo Kα ($\lambda = 0.71069$ Å) radiation. The structures were directly solved and the parameters were refined in the CrystalStructure program package.[41] Numerical absorption correction was used. All of the hydrogen atoms were found experimentally for phpyNOH and phpyNO. Thermal displacement parameters were refined anisotropically for non-hydrogen atoms and those of hydrogen atoms were treated isotropically. The hydrogen atoms in **1**−**4** were placed at calculated positions, and their parameters were refined as "riding." Selected crystallographic data are summarized in Table 5.

Magnetic Susceptibility. Magnetic susceptibilities of the polycrystalline samples of the present complexes were measured on a Quantum Design MPMS SQUID magnetometer at an applied magnetic field of 500 Oe in a temperature range down to 1.8 K. The magnetic response was corrected with diamagnetic blank data of the sample holder obtained separately. The diamagnetic contribution of the sample itself was estimated from Pascal's constant.

Molecular Orbital Calculation. Molecular orbital calculations were performed with the Gaussian03 program.[42] We applied unrestricted density functional (DFT) UB3LYP methods with the Becke exchange functional[43] and the Lee−Yang−Parr correlation functional.[44] The 6−311G(d,p) basis set was chosen. The convergence criterion for the energy was set at 10^{-9} a.u. Calculations of phpyNO and 2pyNO were done after geometrical optimization with the same method using the 6−31G(d,p) basis set. For the calculation on a model compound (Figure 7), we applied a conformation analysis routine in the Spartan'02 program.[45] The molecular geometry was fully optimized on the restricted HF/3−21G level except for the constraint of the $Cu-O-N-C_{2py}$ dihedral angle. The calculation points were set to $\phi = 0-35°$ with an interval of 5°. The energies of the triplet and broken-symmetry singlet[46] states were calculated at the UB3LYP/6−311G(d,p) level with the Gaussian03 program. The convergence criterion for the energy was set at 10^{-9} a.u.

Acknowledgment. This work was supported by Grants-in-Aid for Scientific Research (Nos. 15073101, 17550166, and 19550135) from the Ministry of Education, Culture, Sports, Science, and Technology, Japan.

Supporting Information Available: CIF files including selected geometrical parameter tables for phpyNOH, phpyNO, **1**, **2**, **3**, and **4**. This material is available free of charge via the Internet at http://pubs.acs.org.

IC800937N

(40) *WinEPR Simfonia*, version 1.25; Bruker Biospin: Rheinstetten, Germany, 1996.
(41) *CrystalStructure*, version 3.8; Rigaku/MSC: The Woodlands, TX, 2000−2006.
(42) Frisch, M. J.; Trucks, G. W.; Schlegel, H. B.; Scuseria, G. E.; Robb, M. A.; Cheeseman, J. R.; Montgomery, J. R., Jr.; Vreven, T.; Kudin, K. N.; Burant, J. C.; Millam, J. M.; Iyengar, S. S.; Tomasi, J.; Barone, V.; Mennucci, B.; Cossi, M.; Scalmani, G.; Rega, N.; Petersson, G. A.; Nakatsuji, H.; Hada, M.; Ehara, M.; Toyota, K.; Fukuda, R.; Hasegawa, J.; Ishida, M.; Nakajima, T.; Honda, Y.; Kitao, O.; Nakai, H.; Klene, M.; Li, X.; Knox, J. E.; Hratchian, H. P.; Cross, J. B.; Adamo, C.; Jaramillo, J.; Gomperts, R.; Stratmann, R. E.; Yazyev, O.; Austin, A. J.; Cammi, R.; Pomelli, C.; Ochterski, J. W.; Ayala, P. Y.; Morokuma, K.; Voth, G. A.; Salvador, P.; Dannenberg, J. J.; Zakrzewski, V. G.; Dapprich, S.; Daniels, A. D.; Strain, M. C.; Farkas, O.; Malick, D. K.; Rabuck, A. D.; Raghavachari, K.; Foresman, J. B.; Ortiz, J. V.; Cui, Q.; Baboul, A. G.; Clifford, S.; Cioslowski, J.; Stefanov, B. B.; Liu, G.; Liashenko, A.; Piskorz, P.; Komaromi, I.; Martin, R.L.; Fox, D. J.; Keith, T.; Al-Laham, M. A.; Peng, C. Y.; Nanayakkara, A.; Challacombe, M.; Gill, P. M. W.; Johnson, B.; Chen, W.; Wong, M. W.; Gonzalez, C.; Pople, J. A. *Gaussian03*, revision C.02; Gaussian, Inc.: Wallingford, CT, 2004.
(43) Becke, A. D. *J. Chem. Phys.* **1993**, *98*, 5648.
(44) Lee, C.; Yang, W.; Parr, R. G. *Phys. Rev. B* **1998**, *37*, 785.
(45) *SPARTAN'02*; Wavefunction Inc.: Irvine, CA, 2002.
(46) Ruiz, E.; Cano, J.; Alvarez, S.; Alemany, P. *J. Comput. Chem.* **1999**, *20*, 1391.